Chapter 2

Inhibition of Vascular Endothelial Growth Factor with a Sequence-Specific HRE Antagonist

The text of this chapter is taken in part from two manuscripts. The first is coauthored with Bogdan Z. Olenyuk, Guo-Jun Zhang, Jeffery M. Klco, William G. Kaelin, Jr., and Peter B. Dervan. The second is coauthored with Claire S. Jacobs, Michelle E. Farkas, and Peter B. Dervan.

(Olenyuk, B. Z., Zhang, G. J., Klco, J. M., Nickols, N. G., Kaelin, W. G. and Dervan, P. B. (2004) *Proc. Natl. Acad. Sci. U. S. A.* **101,** 16768-16773.)

(Nickols, N. G., Jacobs, C. S., Farkas, M. E. and Dervan, P. B. (2007) *Nucleic Acids Res.* **35,** 363-370.)

Abstract

Vascular endothelial growth factor (VEGF) and its receptors have been implicated as key factors in tumor angiogenesis that is upregulated by chronic hypoxia. We evaluated the effects of DNA-binding small molecules on hypoxia-inducible transcription of VEGF. A synthetic pyrrole-imidazole polyamide designed to bind the hypoxia response element (HRE) was found to disrupt hypoxia-inducible factor (HIF) binding to the HRE. In cultured HeLa cells this resulted in a reduction of VEGF mRNA and secreted protein levels. Occupancy at the VEGF HRE was decreased in the presence of the polyamide. The observed effects were polyamide specific and dose dependent. Analysis of genome-wide effects of the HRE-specific polyamide revealed that a number of hypoxia-inducible genes were downregulated. In addition, siRNA targeted against HIF-1α had an effect on VEGF expression that was comparable to that of the polyamide. The pathway-based regulation of hypoxia-inducible gene expression with DNA-binding small molecules may represent a new approach for targeting angiogenesis.

2.1 Introduction

Angiogenesis, the induction of new blood vessels, is critical for growth and metastatic spread of solid tumors. It is tightly controlled by a number of specific mitogenic factors among which vascular endothelial growth factor (VEGF) and its receptors play a central role. The levels of VEGF are upregulated across a broad range of tumors and are involved in key aspects of cancer biology. A hallmark of many cancers, chronic hypoxia, in conjunction with activation of certain oncogenic signaling pathways, is responsible for the elevated levels of VEGF and is associated with invasion and altered energy metabolism (1).

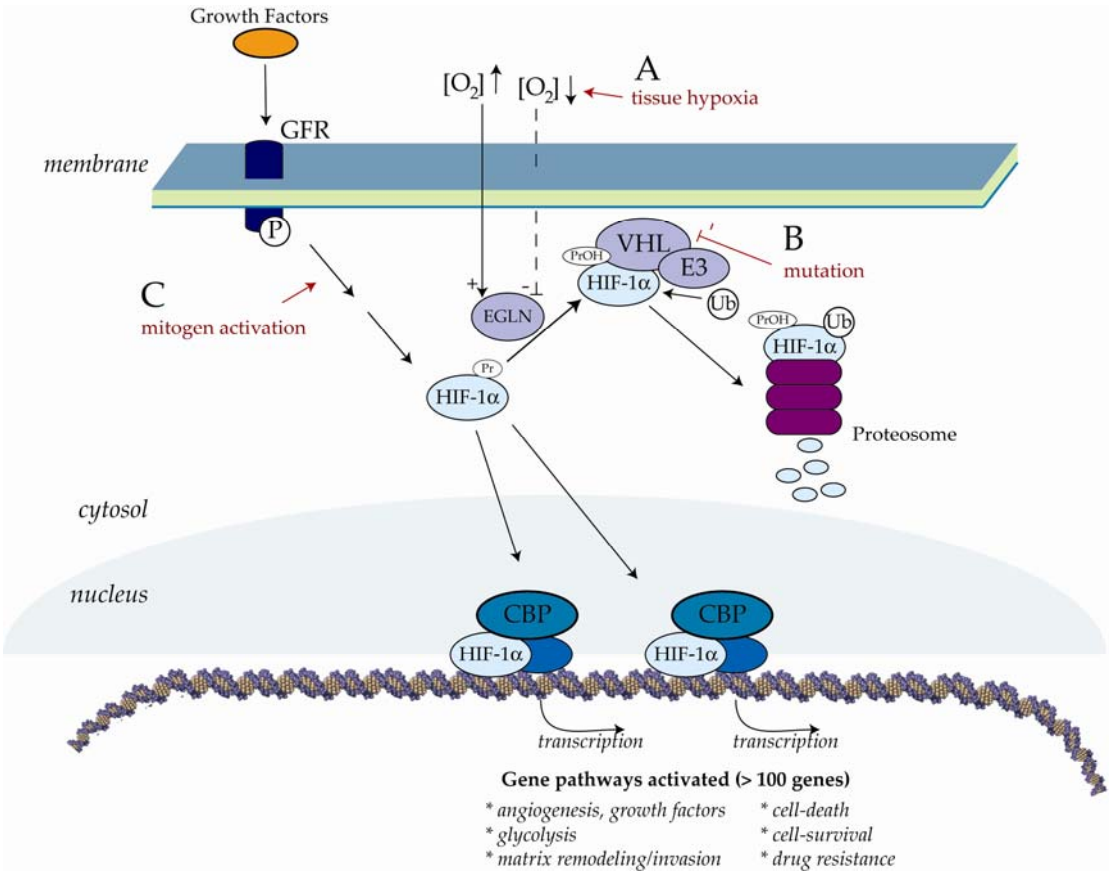

Figure 2.1 Regulation of HIF-1 activity. Under normoxia, HIF-1α is hydroxylated, ubiquitinated, and degraded. HIF-1 activation in tumors can occur through: (A) decreased O_2 in a hypoxic tumor microenvironment (B) inactivating mutations in VHL, or (C) activation by upstream growth signals.

In cells and tissues, hypoxia triggers a multifaceted adaptive response that is primarily driven by the heterodimeric hypoxia-inducible factor 1 (HIF-1) (Figure 2.1) (2). Under normal dioxygen levels, the α-subunit of HIF-1 is successively hydroxylated at proline residue 564 (3), ubiquitinated, and then degraded by the ubiquitin-proteosome system. This process, mediated by the von Hippel-Lindau tumor suppressor protein (4), is responsible for controlling levels of HIF-1α and, as a result, the transcriptional response to hypoxia (5). Under hypoxic conditions, HIF-1α avoids hydroxylation and accumulates. Heterodimerization with its constitutively expressed binding partner, aryl hydrocarbon receptor nuclear translocator (ARNT) (6), and binding to a cognate hypoxia response element (HRE) (7) recruits the p300/CBP and SRC-1 family co-activators, which drive the expression of hypoxia-inducible genes. Among these are genes encoding angiogenic peptides such as VEGF and the PDGF B chain, as well as proteins involved in glucose metabolism such as the GLUT1 glucose transporter (8, 9). Inhibition of VEGF, a downstream target of HIF, is sufficient to inhibit tumor growth in model systems (10). In tumors, HIF-1 can result from a hypoxic microenvironment, deactivating mutations in VHL, or activation by signaling through growth factors and mTOR (Figure 2.1).

We designed a sequence-specific DNA binding molecule to inhibit binding of the HIF-1α/ARNT heterodimer to its cognate DNA sequence in order to down-regulate the expression of VEGF and other hypoxia-inducible genes. Because interaction of HIF with its cognate DNA sequence and subsequent transcriptional activation is a likely point of significant amplification of response, disruption of this interaction could represent a point of intervention in the hypoxia response pathway involving multiple genes.

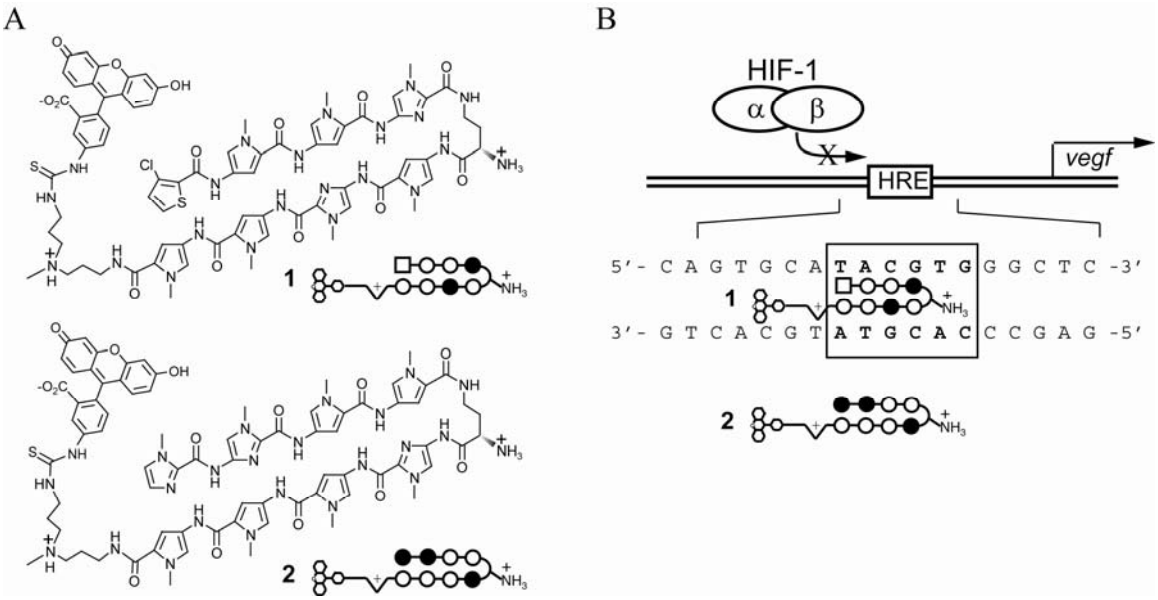

Figure 2.2 Structure of polyamides used in this study. (A) Structures of the polyamide-FITC conjugates **1-2**. Imidazole and pyrrole rings are represented as solid and open circles, respectively; 3-chlorothiophene is depicted as a square, aliphatic linkers as curved lines. Half-diamonds with plus signs represent 3,3'-diamino-*N*-methyl-dipropylamine. (B) Map of the VEGF promoter with the HRE site (top) and schematic representation of match polyamide **1** targeting the HRE and mismatch polyamide **2** designed for this study (bottom).

In order to regulate the expression of endogenous genes, DNA-binding small molecules must permeate the cell, localize in the nucleus (11, 12), access chromatin (13-15) and bind DNA sequences with affinities and specificities sufficient to disrupt key regulatory proteins within genomic DNA (16-18). Synthetic oligomers containing *N*-methylpyrrole (Py) and *N*-methylimidazole (Im) amino acids conjugated to a fluorescein dye represent a modular molecular recognition toolkit with properties that satisfy these criteria. DNA sequence specificity is programmed by a simple code created by pairs of aromatic rings (19-22).

Although the VEGF gene encodes multiple splicing variants, analysis of its promoter revealed that a single hypoxia response element (HRE) is located at nucleotide positions -947 to -939 (5'-TACGTG-3') relative to the common transcription start site

(Figure 2.2) (23). We designed polyamide **1** to bind to the DNA sequence 5'-WTWCGW-3' (where W = A or T) that encompasses the HRE site in the VEGF promoter according to the pairing rules (figure 2.2). A mismatch control polyamide **2**, directed against an unrelated sequence 5'-WGGWCW-3', was also synthesized.

2.2 Materials and methods

Synthesis of polyamides. Polyamides **1** and **2** were synthesized by solid-phase methods on Kaiser oxime resin (Nova Biochem, Laufelfingen, Switzerland) (24) and conjugated to fluorescein isothiocyanate, isomer I (FITC) (11). The purity and identity of the polyamide-dye conjugates were verified by analytical HPLC, UV-visible spectroscopy, and matrix-assisted laser desorption ionization time-of-flight mass spectrometry (MALDI-TOF MS).

Determination of DNA binding affinities and sequence specificities. A 5' ^{32}P-labeled fragment was generated by PCR amplification of the site from the plasmid pGL2-VEGF-Luc using primers 5'-CTC AGT TCC CTG GCA ACA TCT-3' (VEGFP1) and 5'-TGG CAC CAA GTT TGT GGA GCT-3' (VEGFP2) and isolated by nondenaturing gel electrophoresis (25). Quantitative DNase I footprint titration experiments were used to determine the binding affinities and specificities of polyamides **1** and **2** (25).

Electrophoretic mobility shift assays. The HIF1α/ARNT heterodimer was transcribed/translated *in vitro* using Promega TNT kit according to the manufacturer's instructions. The double-strand oligonucleotide probe was prepared by annealing the two complementary strands 5'-GAC TCC ACA GTG CAT ACG TGG GCT CCA ACA GGT-3' (HRE-EMSA1) and 5'-ACC TGT TGG AGC CCA CGT ATG CAC TGT GGA

GTC-3' (HRE-EMSA2). Before annealing, the HRE-EMSA1 oligonucleotide was 5'-end radiolabeled with γ-^{32}P-ATP (NEN) and T4 polynucleotide kinase as described previously. The radiolabeled double-strand oligonucleotide probe was isolated using a G25 Quickspin column (Boehringer Mannheim).

Polyamides were preincubated with the radiolabeled oligonucleotide in Z-buffer (100 mM KCl, 25 mM Tris, pH 7.5, 0.2 mM EDTA, 20% glycerol, 0.25 mg/ml BSA, 0.05% NP-40, 5 mM DTT, 0.1 mg/ml PMSF and 1.2 mM sodium vanadate) at 0°C for 30 min. Then the *in vitro* transcribed/translated protein mixture, diluted with the same buffer, was added, and the mixture was held on ice for an additional 30 min. Each time, the following controls were included: free oligonucleotide probe, probe with unprogrammed *in vitro* transcription/translation reaction mixture, and 100-fold excess of competing non-radiolabeled probe. The complexes were resolved on a 4% non-denaturing polyacrylamide gel and visualized with the Storm 820 Phosphorimager (Molecular Dynamics).

Cell culture. The human cervical epithelial adenocarcinoma cell line HeLa (American Type Culture Collection CCL-2) was maintained in Dulbecco's Modified Eagle's Medium (DMEM) as recommended by ATCC. Cell growth and morphology were monitored by phase-contrast microscopy.

Confocal microscopy. HeLa cells were trypsinized for 5–10 min at 37°C, centrifuged for 5 min at 2,000 rpm and 5°C in a Beckman-Coulter Allegra 6R centrifuge, and resuspended in fresh medium to a concentration of 1.25×10^6 cells per ml. Incubations were performed by adding 150 μl of cells into culture dishes equipped with glass bottoms for direct imaging (MatTek, Ashland, MA). The cells were grown in the glass-bottom

culture dishes for 24 h. The medium was then removed and replaced with 142.5 μl of fresh medium. Then 7.5 μl of the 100 μM polyamide solution was added and the cells were incubated in a 5% CO_2 atmosphere at 37°C for 10–14 h. Imaging was performed on a Zeiss LSM 5 Pascal inverted laser scanning microscope equipped with a ×40 oil-immersion objective lens. Analysis of images was performed as previously described (11).

Determination of relative mRNA and protein levels.

RNA isolation. HeLa cells were plated in 6-well dishes at a density of 6×10^4 in 1 ml of DMEM and allowed to attach for 16–20 h. Polyamides were added and the cells were incubated for 48 h. The hypoxia conditions necessary for VEGF induction were created by incubation with 300 μM desferrioxamine mesylate (DFO) for 16–18 h (26, 27). Optionally, cells were tested for apoptosis by staining with Annexin V. The medium was removed, cells were washed with ice-cold PBS and immediately lysed with RLT buffer from the RNeasy kit (Qiagen) with 2-mercaptoethanol added. Further RNA isolation was carried out with the RNeasy kit as described in the manufacturer's manual. The isolated total RNA was quantified. The yields were 12–15 μg per well. Genomic DNA was digested by treatment with DNase I from a DNA Free kit (Ambion) and DNase I was inactivated with bead-immobilized DNase I inactivation reagent (Ambion). HIF-1α siRNA (HIF-1α validated duplex #1, Invitrogen) was transfected using Lipofectamine 2000 according to the manufacturer's (Invitrogen) instructions.

Reverse transcription. A 2.5 μg sample of total RNA was used to reverse-transcribe cDNA using Powerscript II reverse transcriptase (BD Clontech) according to

the manufacturer's protocol. Random hexamers and oligo-$(dT)_{16}$ primers were used simultaneously in a 1:1 ratio. The total volume for each RT reaction was 20 μl.

Real-time quantitative RT-PCR analysis was performed using the VEGF gene primers described below. The forward primer 5'-AGG CCA GCA CAT AGG AGA GA-3' and reverse primer 5'-TTT CCC TTT CCT CGA ACT GA-3' were used to amplify the 104-bp fragment from the 3'-translated region of VEGF. RNA was standardized by quantification of the β-glucuronidase gene as an endogenous control (28). The forward primer 5'-CTC ATT TGG AAT TTT GCC GAT T and reverse primer 5'- CCG AGT GAA GAT CCC CTT TTT A were used for this gene (29). Quantitative real-time RT-PCR was performed using Applied Biosystems SYBR Green RT-PCR master mix according to the manufacturer's instructions. Temperature cycling and detection of the SYBR Green emission were performed with an ABI 7300 real-time instrument using Applied Biosystems Sequence Detection System version 1.2. Statistical analysis was performed on three independent experiments.

VEGF ELISA. Approximately 10^5 HeLa cells were split into 24-well plates. After 24 h, the cells were incubated with polyamides **1** or **2** (0.2 μM or 1 μM) for 32 h. Fresh polyamide was added followed by addition of DFO (300 μM) and further incubation for 16 h. The supernatant (100 μl) was used for the VEGF ELISA (RandD) which was carried out according to the manufacturer's instructions.

Analysis of Gene Expression with Oligonucleotide Microarrays. Experiments were carried out at the Caltech Genome Expression Center. HeLa cells were split and plated in a manner similar to that in the RT-PCR experiments. Cultured cells were incubated for 48 h with 0.2 μM or 1 μM polyamide **1** or **2**. Hypoxic conditions were induced by

adding DFO to a final concentration of 300 μM. The cells were incubated with DFO for 12 h and total RNA was collected as described for the RT-PCR experiments. After testing for quantity and quality, the total RNA was subjected to the Affymetrix protocols. Affymetrix Genechip® Human Genome U133A microarrays were used in each experiment. The experiments were carried out in triplicate. Correlation between the replicates was greater than 0.970. The data were analyzed with Resolver 3.0 from Rosetta Biosoftware.

2.3 Results

Binding affinities and specificities. Based on the pairing rules, match polyamide **1** targets sequences of the type 5'- WTWCGW -3' (where W = A or T), whereas mismatch polyamide **2** targets sequences of the type 5'- WGGWCW-3'. The 3-chlorothiophene ring at the N-terminus of polyamide **1** provides specificity for a T•A base pair (22). We mapped the detailed binding sites for both match and mismatch polyamides on the VEGF promoter fragment that encompasses the HRE. From DNase I footprint titrations, a K_a value of 6.3×10^9 M^{-1} was obtained for polyamide **1** at the HRE site (Figure 2.3A). The mismatch polyamide **2** bound the HRE site with ~100-fold lower affinity ($K_a = 7.9 \times 10^7$ M^{-1}). No match sites could be found for polyamide **2** in the region of this DNA that can be resolved by gel electrophoresis. High sequence specificity was observed for both polyamides despite the presence of the conjugated fluorescein moiety.

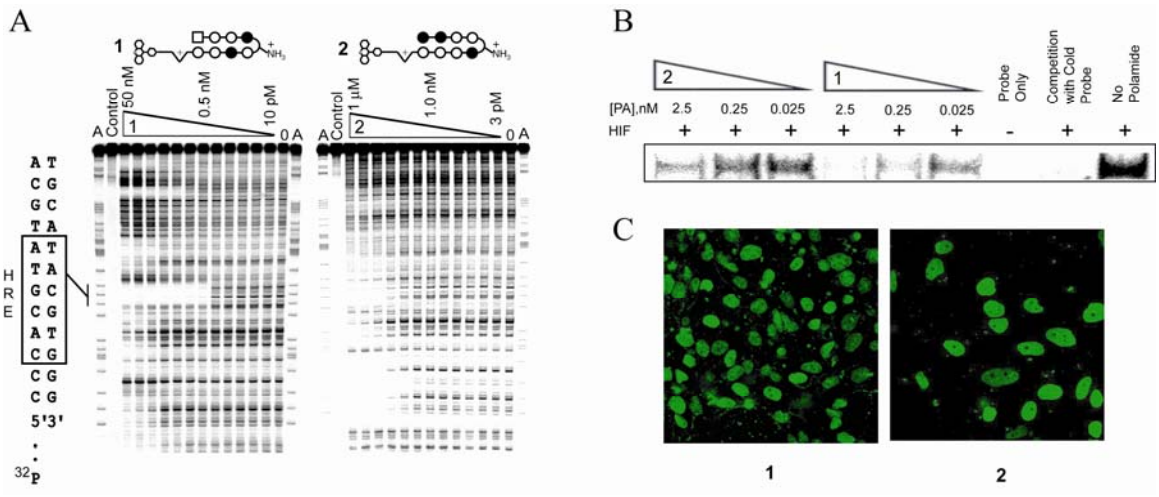

Figure 2.3 (A) Storage phosphor autoradiograms from quantitative DNase I footprint titrations of polyamides **1** and **2**. The boxed sequence on the left represents the HRE site. For polyamide **1**, lanes 1 and 16, A reaction; lane 2, intact DNA; lanes 3-14, DNase I digestion products in the presence of 50 nM, 20 nM, 10 nM, 5 nM, 2 nM, 1 nM, 500 pM, 200 pM, 100 pM, 50 pM, 20 pM, 10 pM polyamide respectively; lane 15, DNase I standard. For polyamide **2**, lanes 1 and 16, A reaction; lane 2, intact DNA; lanes 3-14, DNase I digestion products in the presence of 1 μM, 300 nM, 100 nM, 30 nM, 10 nM, 3 nM, 1 nM, 300 pM, 100 pM, 30 pM, 10 pM, 3 pM polyamide respectively; lane 15, DNase I standard. (B) Storage phosphor autoradiogram from EMSA experiment with polyamides **1** and **2**. (C) Cellular localization of polyamide **1** (left) and **2** (right) in live HeLa cells.

Disruption of the HIF-DNA complex. We tested the ability of polyamides to inhibit the binding of HIF-1α/ARNT heterodimer to the HRE in an electrophoretic mobility shift assay (EMSA). The radiolabeled DNA fragment (24-bp) was first incubated with match or mismatch polyamide **1** or **2**, respectively. After the subsequent addition of the *in vitro* translated HIF-1α/ARNT heterodimer, the resulting complexes were resolved on a nondenaturing polyacrylamide gel. Match polyamide **1** (0.25 μM) effectively inhibited binding of the heterodimer, whereas much less effect was observed for the mismatch polyamide **2** at concentrations as high as 2.5 μM (Figure 2.3B).

Uptake of polyamides in cultured HeLa cells. The uptake of both polyamides by the HeLa cell line was examined by laser-scanning confocal microscopy. Previous studies

indicated that the degree of cellular uptake and nuclear localization of polyamides containing an eight-ring sequence recognition core is dependent on the pyrrole/imidazole content of the core and varies for each cell line (11, 12). We find that both polyamides exhibit strong nuclear localization after incubation at 2 μM concentration for 12 h at 37 °C in standard culture medium (Figure 2.3C).

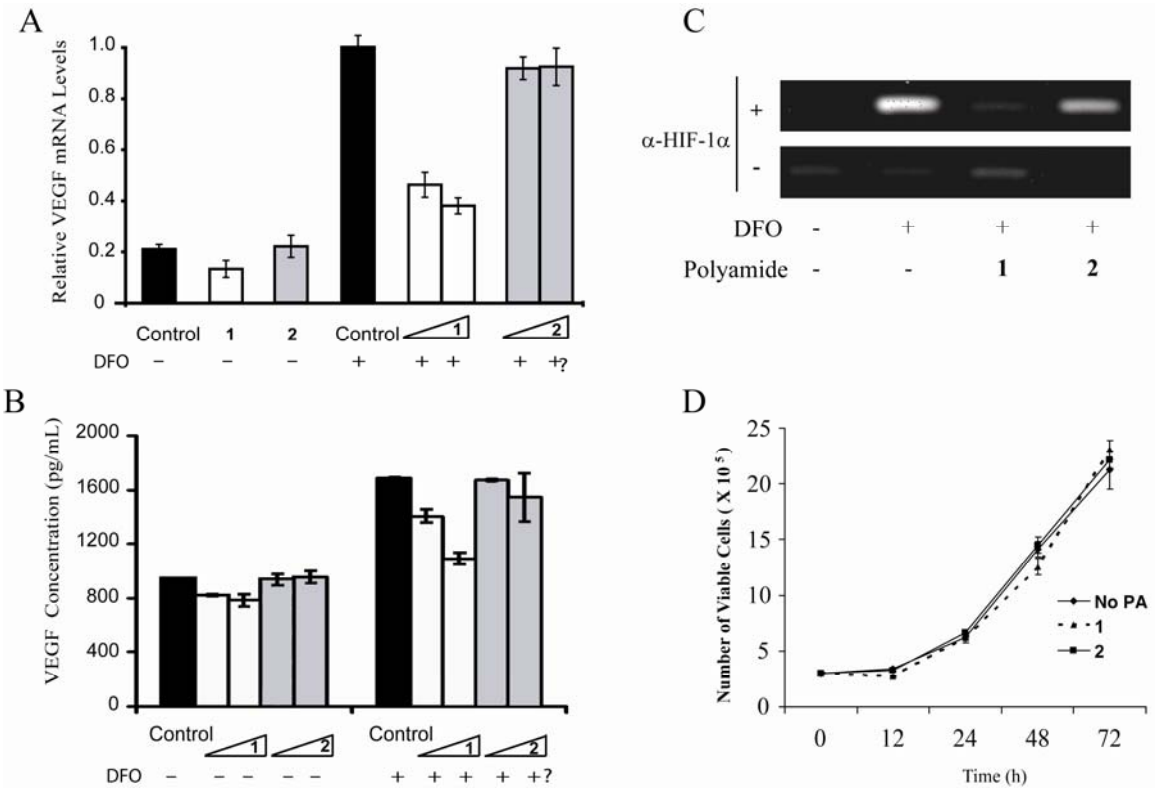

Figure 2.4 (A) Relative mRNA levels of expression of the VEGF gene as measured by real-time quantitative RT-PCR. (B) Levels of secreted VEGF protein as measured by ELISA. The final concentration of polyamides **1** and **2** was 0.2 μM or 1 μM. Non-induced polyamide concentrations in (A) were 1 μM for each. (C) Chromatin immunoprecipitation at the VEGF HRE under the designated conditions. HIF-1α occupancy the VEGF HRE is inhibited by **1** and to a lesser degree, **2**. (D) Number of viable cells. Data represent three independent experiments. Polyamide concentrations are 1 μM in (C) and (D).

Effect of polyamides on cell viability and growth rate. We examined whether prolonged incubation with polyamides affects cell viability. HeLa cells were incubated

with polyamides at 1 μM concentration, trypsinized and counted at various time points (0-72 h) using a hemocytometer. Measurements of cell growth rates indicate that polyamides at 1 μM in standard culture medium have no deleterious effects on cell growth and division (Figure 2.4D).

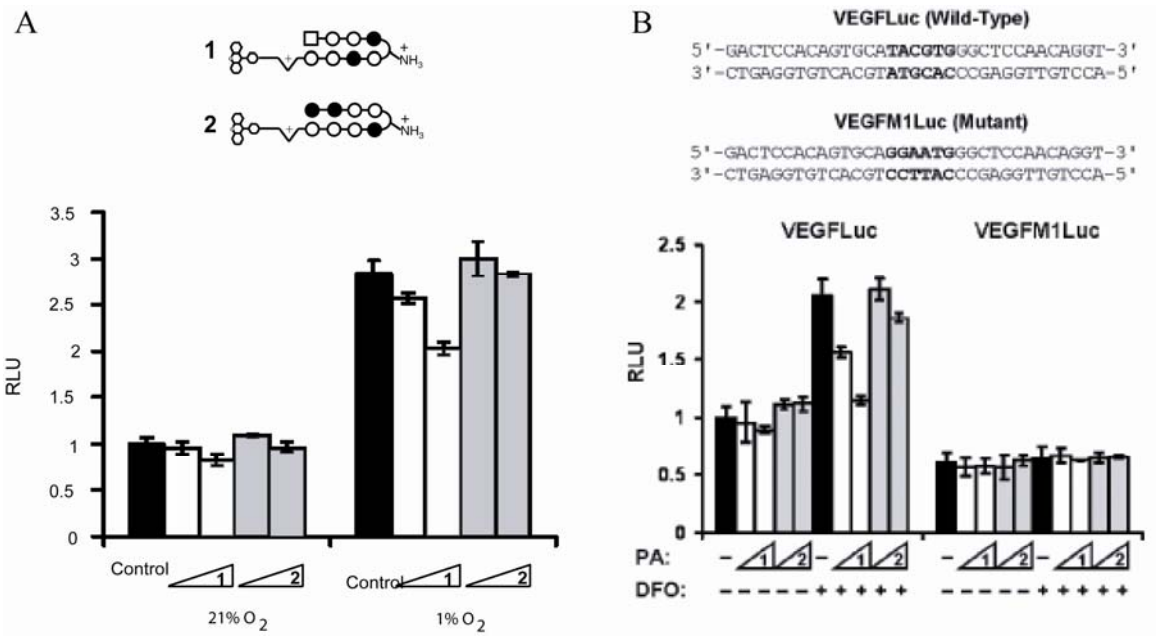

Figure 2.5 (A) Inhibition of the expression of a VEGF-Luc reporter gene under physiological hypoxia. HeLa cells, stably transfected with plasmids encoding firefly luciferase driven by wild-type (pGL3-VEGF-Luc) were split into 24 well plates. After 24 h, the cells were incubated with polyamides **1** or **2** (0.2 or 1 μM) for a further 48 h. The cells were incubated in a hypoxia chamber supplied with 1% oxygen for 16 h followed by harvesting with PLB buffer (Promega). Luciferase activity was measured according to the manufacturer's instructions. (B) Inhibition of the expression of wild-type VEGF-Luc and mutated VEGF-M1Luc reporter genes. Cells were induced with 300 μM DFO. The concentration of polyamides **1** and **2** was 0.2 μM or 1 μM.

Suppression of hypoxia-inducible transcription in cultured cells. We utilized real-time quantitative RT-PCR assays to evaluate the relative levels of VEGF mRNA in hypoxic HeLa cells treated with polyamides. In parallel, untreated cells were used as controls. Expression of β-glucuronidase was used as a control gene for determining the

relative levels of transcription (29). After 48 h of incubation with polyamide **1**, levels of VEGF expression were reduced in a dose-dependent manner (Figure 2.4A). Polyamide **1** at 1 μM inhibits VEGF expression approximately 60%, which is near the VEGF levels in the uninduced (normoxic) cells. Mismatch polyamide **2** shows minimal inhibition at either 0.2 μM or 1 μM concentrations.

ELISA was used to determine the levels of secreted VEGF. Total protein levels were monitored in parallel, to exclude the possibility of disruption of general transcriptional activity by the polyamides. Under normoxia, match polyamide **1** caused a modest decrease of the basal expression levels of VEGF whereas mismatch polyamide **2** caused no decrease of VEGF levels. Under hypoxic conditions, polyamide **1** decreased levels of VEGF in a dose-dependent manner, whereas mismatch polyamide **2** had a minimal effect (Figure 2.4B).

Analysis of promoter activity with luciferase assays. We used HeLa cells that had been stably transfected with a reporter plasmid VEGF-Luc containing the VEGF promoter fused to luciferase. The experiments were carried out in a hypoxic chamber with 1% O_2 to mimic closely the conditions of physiological hypoxia. Incubation with the match polyamide **1** resulted in a decrease of promoter activity in a dose-dependent manner as indicated by decreased levels of luciferase activity (Figure 2.5A). A negligibly small effect was observed for mismatch polyamide **2**.

As a specificity control, we constructed and used in parallel a nearly identical reporter VEGF-M1Luc where the HRE and surrounding sequences had been mutated to disfavor binding of HIF-1 (Figure 2.5B). In these experiments and those that follow, the hypoxia mimetic compound desferrioxamine mesylate (DFO) (26, 27) was used to

stabilize HIF and activate HIF target genes. Cells were harvested after incubation with 300 μM DFO for 12-16 hours.

Treatment of stably transfected HeLa cells with match polyamide **1** led to significant attenuation of hypoxia-inducible VEFG-Luc activity. By contrast, treatment with mismatch polyamide **2** resulted in only a modest decrease of VEGF-Luc activity. The VEGF-M1Luc promoter with a mutated HRE site showed no inducibility under hypoxic conditions. No effect of polyamides on the levels of luciferase activity in cells transfected with the mutant promoter was observed (Figure 2.5B). No obvious cytotoxicity was observed.

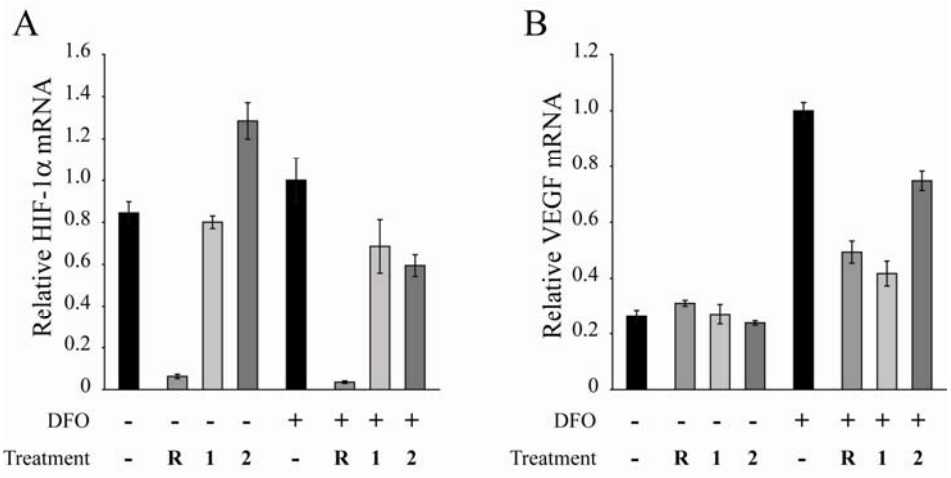

Figure 2.6 (A) siRNA against HIF-1α (**R**) decreases HIF-1α mRNA by more than 95% under DFO-induced and non-induced conditions in HeLa cells. **1** and **2** have modest affects on HIF-1α expression. (B) siRNA against HIF-1α has a comparable affect to **1** on DFO-induced VEGF expression.

To establish a benchmark of comparison to a theoretical maximum level of inhibition possible through disruption of the HIF-1-DNA interface at the VEGF HRE, siRNA was used to silence expression of HIF-1α (Figure2.6A). DFO-induced VEGF expression was inhibited by approximately 50% by the siRNA (Figure 2.6B), which is

comparable to the effect observed for polyamide **1** under the conditions of this experiment.

Genome-wide effects of polyamides. The effects of polyamide treatment on nuclear transcription were monitored by global gene expression analysis using Affymetrix high-density UniGene 133A microarrays, which contain oligonucleotide sequences representing over 20,000 annotated genes. HeLa cells were treated in triplicate with no polyamide, polyamide **1**, or polyamide **2** at 1 μM and 0.2 μM concentrations, for 48 hours. DFO was then added to a concentration of 300 μM for an additional 12-16 hours and total RNA was collected. Purified RNA was treated and hybridized to the oligonucleotide microarrays according to established protocols.

Figure 2.7 lists the number of genes affected uniquely and similarly by polyamides **1** and **2** at 0.2 μM and 1 μM. At each threshold there is a majority of genes uniquely affected by each polyamide, as well as a number of genes similarly affected by both polyamides. This is consistent with previous work suggesting that polyamides that target different DNA sequences can affect the expression of different sets of genes (13). At a threshold of 2.0-fold, 264 and 73 genes are downregulated and upregulated, respectively, in the presence of polyamide **1** at 1 μM. This represents only 1.5% of the interrogated genes. In the case of polyamide **2**, less than 1.0% are affected at this threshold. These effects are surprising given that a polyamide with a six basepair binding site is expected to have more than 1.4 million match sites in a 3 billion basepair genome. Polyamides **1** and **2** at 0.2 μM affect the expression of fewer genes at each threshold level as compared to the 1 μM data sets. It should be noted that most genes downregulated and

upregulated by each polyamide at 0.2 μM are similarly affected in the 1 μM data set for each polyamide.

Table 2.1 Relative expression levels of selected HIF-inducible genes.

Genbank ID	Annotated Gene	Fold Change			
		1 (1 μM)	**1** (0.2 μM)	**2** (1 μM)	**2** (0.2 μM)
	Energy Metabolism				
AI761561	Hexokinase-2	-1.3	–	–	–
NM_005165.1	Aldolase-C	–	–	–	–
	Hormones/Receptors				
J03241.1	Transforming Growth Factor β3	–	–	–	–
	Vasoactive Proteins				
AF022375.1	VEGF	-1.35	-1.4	–	–
NM_002019.1	VEGF Receptor, Flt-1	-1.5	–	–	–
NM_001955.1	Endothelin-1	-2.4	-1.9	-1.3	–
NM_001956.1	Endothelin-2	-13.2	-2.2	-2.8	-2.0
NM_000114.1	Endothelin-3	-1.8	–	–	–

Next, we analyzed differential expression levels of several hypoxia-inducible genes in the presence of polyamides **1** or **2** (Table 2.1). The expression of the main target gene, VEGF, is downregulated by 1.34 fold with polyamide **1** and virtually unaltered with polyamide **2**. These data parallel the RT-PCR experiments and luciferase experiments. Other hypoxia-inducible genes are also affected, albeit to a different extent. Remarkably, the microarray data indicated significantly downregulated levels of the mRNAs corresponding to all three endothelin genes. In fact, the levels of endothelin-2 (ET-2) were over 90% (13.6 fold) downregulated with polyamide **1** as compared to the untreated controls. Interestingly, the controls treated with polyamide **2** show nearly 3-fold downregulation of ET-2. This effect was validated by real-time quantitative RT-

PCR of ET-2 mRNA levels, where 6.8 fold downregulation was observed for polyamide **1** and 2.4 fold for polyamide **2** (Figure 2.8A). According to the microarray data, ET-1 was found to be downregulated 2.4 fold by polyamide **1** and 1.26 fold by polyamide **2**. Real-time quantitative RT-PCR measurements were generally consistent with a 1.5 fold downregulation of ET-1 mRNA by polyamide **1** and no detectable downregulation by polyamide **2**. Recent studies indicate the emerging role of endothelins in cancer (30). In addition, ET-2 has been recently implicated as an autocrine survival factor and a contributor to invasion and metastasis of hypoxic breast cancer cells (31). For this reason, we measured the effects of **1** and **2** on endothelin 2 expression in MCF7 cells (Figure 2.8B). Interestingly, VEGF expression was minimally affected by **1** in MCF7 at **1** μM (data not shown), while endothelin-2 was down-regulated approximately 70% (Figure 2.8B). We will defer a detailed discussion of the effects of polyamides **1** and **2** on the expression of the endothelin genes until a more thorough analysis of their regulation has been undertaken. The effects of **1** and **2** on VEGF expression was also measured in the lung carcinoma cell line A549 (Figure 2.9).

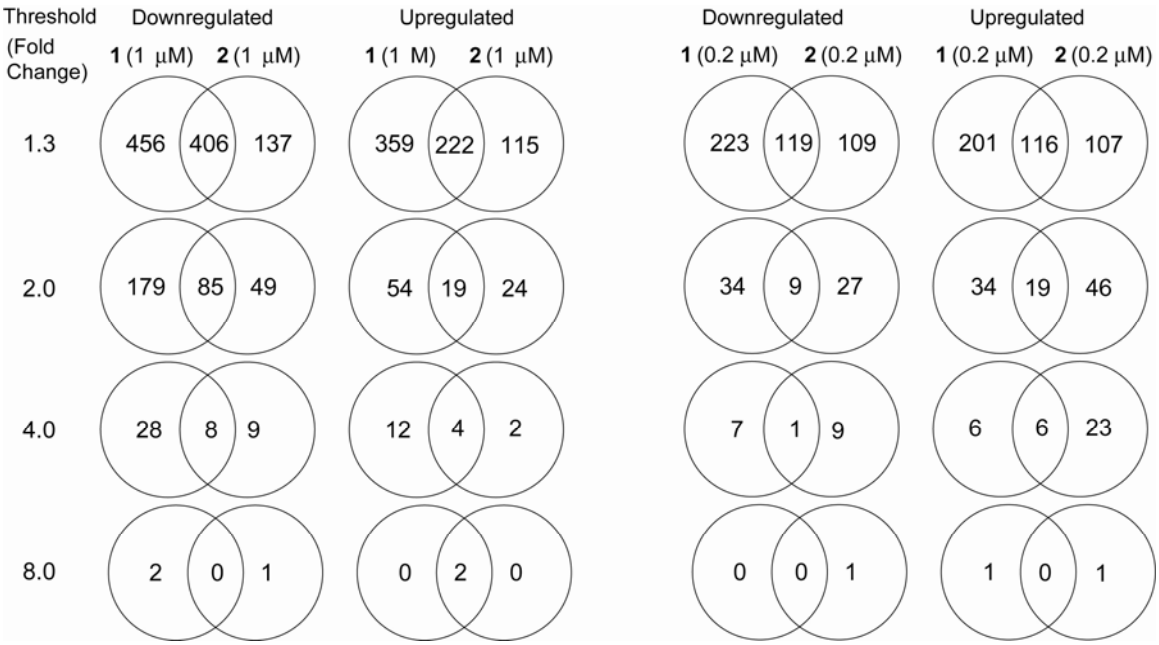

Figure 2.7 Venn diagrams representing the distribution of affected genes ($p < 0.01$) from the microarray experiments. The numbers outside the intersections represent genes uniquely affected by the individual polyamides.

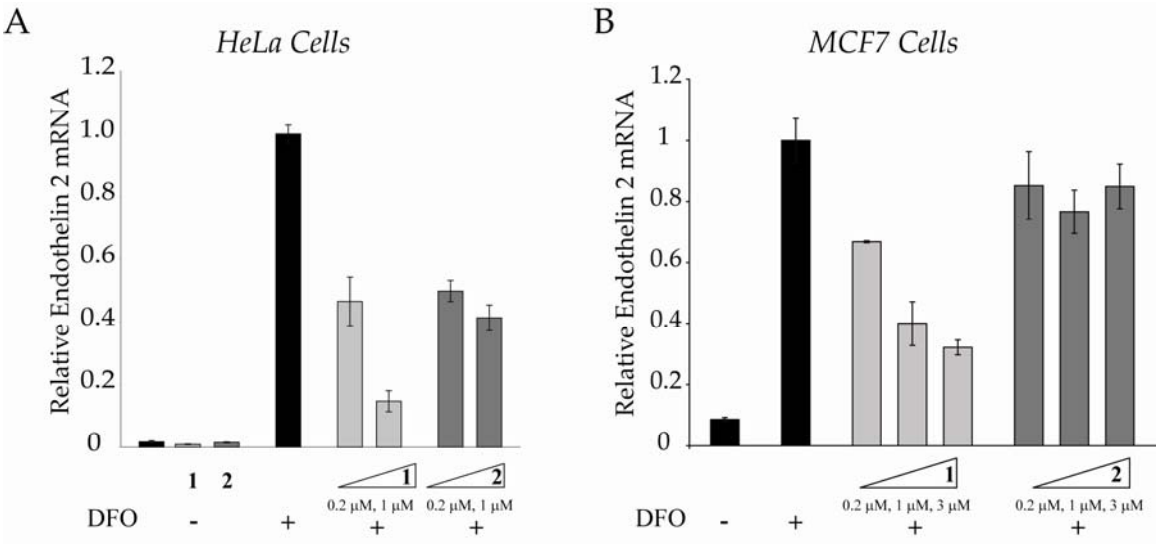

Figure 2.8 Relative mRNA levels of expression of the endothelin 2 gene as measured by real-time quantitative RT-PCR in HeLa (A) and the breast cancer cell line MCF7 (B). Significantly, endothelin 2 has been implicated as an autocrine survival factor and mediator of metastasis and invasion in breast cancer.

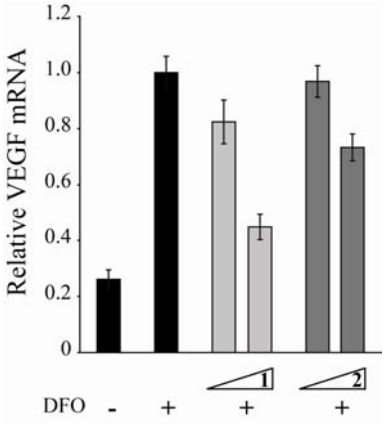

Figure 2.9 (A) Relative mRNA levels of expression of the VEGF gene as measured by real-time quantitative RT-PCR in A549 (lung carcinoma) cells. The final concentration of polyamides **1** and **2** was 0.2 μM or 1 μM.

2.4 Discussion

The expression of VEGF has received considerable attention because this potent mitogen can stimulate endothelial cell proliferation and migration *in vitro* (32, 33) as well as angiogenesis *in vivo* (34, 35). Elevated VEGF levels are associated with the progression of a variety of tumors and correlated to the outcome of cancer treatment (36, 37). To date, numerous attempts to block the activity of VEGF have been made, including the use of antibodies (38), soluble VEGF receptors (39), blocking of the VEGF receptors (40) or degradation of the VEGF message through the use of antisense oligonucleotides (41) or by RNA interference (42, 43). The major focus of the previous studies was inhibition of a single target or a very limited number of targets. This work presents a pathway-specific approach where the expression of multiple genes is downregulated by targeting a common transcription factor binding site. Since there is some sequence variation within the consensus HRE site, we would anticipate that some but not all HIF regulated genes would be affected by polyamide **1** programmed for 5'-WTWCGW-3'.

The details of oncogenic signaling pathways that give rise to the cancerous cellular phenotype continue to be elucidated. These signaling pathways involve a large number of proteins involved in signal transduction that ultimately converge upon a much smaller set of oncogenic transcription factors (44). Hence, targeting transcription factors with small molecules may be the most direct way of reversing the cancerous phenotype. Towards this goal, one can use small molecules to target critical *protein-protein* interactions between transcription factors and coactivators (45, 46). DNA binding polyamides offer an alternate approach by interfering with *protein-DNA* interactions. However, selective gene regulation by programmable DNA binding polyamides depends on a precise knowledge of *cis*-acting promoter elements and the *trans*-acting factors that bind them.

Our results indicate that polyamide-FITC conjugate **1**, designed to target the hypoxia response element (HRE), can bind its cognate site with high affinity and specificity and is capable of disrupting binding of HIF-1 to HRE. The polyamide-FITC conjugate was localized in the nuclei of cultured HeLa cells with no deleterious effects on growth or replication rate. Analysis of the VEGF mRNA levels by real-time quantitative RT-PCR, and secreted levels of VEGF by ELISA, indicated reduction of the promoter activity in hypoxic cells resulting in the concomitant decrease of VEGF production to near its basal levels. Analysis of the genome-wide effects of the polyamide provided further insights into the transcriptional activity of multiple hypoxia-inducible genes. Because many biological responses are threshold-based, the overall decrease of the transcriptional activity to the basal levels could have pronounced downstream effects. Previous studies have shown that the magnitude of induction of VEGF mRNA in mice

subjected to systemic hypoxia varies with tissue type but generally falls between 2- and 4- fold, consistent with the levels of induction measured in this study (47).

Remarkably, Polyamide **1** and siRNA targeted to HIF-1α had a comparable effect on DFO-induced VEGF expression. However, it would be expected that siRNA targeted to HIF-1α would inhibited the hypoxia-induced expression of nearly all HIF-1 regulated genes, while polyamide 1 would target a subset of these genes in a manner consistent with its binding preference and the precise HRE sequences of the HIF-1 target genes. We will defer a more detailed discussion of this comparison until more data are available for analysis.

References

1. Kaelin, W. G. (2002) *Genes Dev.* **16,** 1441-1445.
2. O'Rourke, J. F., Pugh, C. W., Bartlett, S. M. and Ratcliffe, P. J. (1996) *Eur. J. Biochem.* **241,** 403-410.
3. Ivan, M., Kondo, K., Yang, H. F., Kim, W., Valiando, J., Ohh, M., Salic, A., Asara, J. M., Lane, W. S. and Kaelin, W. G. (2001) *Science* **292,** 464-468.
4. Kaelin, W. G. (2002) *Nat. Rev. Cancer* **2,** 673-682.
5. Maxwell, P. H., Wiesener, M. S., Chang, G. W., Clifford, S. C., Vaux, E. C., Cockman, M. E., Wykoff, C. C., Pugh, C. W., Maher, E. R. and Ratcliffe, P. J. (1999) *Nature* **399,** 271-275.
6. Wood, S. M., Gleadle, J. M., Pugh, C. W., Hankinson, O. and Ratcliffe, P. J. (1996) *J. Biol. Chem.* **271,** 15117-15123.
7. O'Rourke, J. F., Dachs, G. U., Gleadle, J. M., Maxwell, P. H., Pugh, C. W., Stratford, I. J., Wood, S. M. and Ratcliffe, P. J. (1997) *Oncol. Res.* **9,** 327-332.
8. Forsythe, J. A., Jiang, B. H., Iyer, N. V., Agani, F., Leung, S. W., Koos, R. D. and Semenza, G. L. (1996) *Mol. Cell. Biol.* **16,** 4604-4613.
9. Okino, S. T., Chichester, C. H. and Whitlock, J. P. (1998) *J. Biol. Chem.* **273,** 23837-23843.
10. Underiner, T. L., Ruggeri, B. and Gingrich, D. E. (2004) *Curr. Med. Chem.* **11,** 731-745.
11. Best, T. P., Edelson, B. S., Nickols, N. G. and Dervan, P. B. (2003) *Proc. Natl. Acad. Sci. U. S. A.* **100,** 12063-12068.

12. Edelson, B. S., Best, T. P., Olenyuk, B., Nickols, N. G., Doss, R. M., Foister, S., Heckel, A. and Dervan, P. B. (2004) *Nucl. Acids. Res.* **32,** 2802-2818.

13. Dudouet, B., Burnett, R., Dickinson, L. A., Wood, M. R., Melander, C., Belitsky, J. M., Edelson, B., Wurtz, N., Briehn, C., Dervan, P. B. and Gottesfeld, J. M. (2003) *Chem. Biol.* **10,** 859-867.

14. Suto, R. K., Edayathumangalam, R. S., White, C. L., Melander, C., Gottesfeld, J. M., Dervan, P. B. and Luger, K. (2003) *J. Mol. Biol.* **326,** 371-380.

15. Edayathumangalam, R. S., Weyermann, P., Gottesfeld, J. M., Dervan, P. B. and Luger, K. (2004) *Proc. Natl. Acad. Sci. U. S. A.* **101,** 6864-6869.

16. Gottesfeld, J. M., Neely, L., Trauger, J. W., Baird, E. E. and Dervan, P. B. (1997) *Nature* **387,** 202-205.

17. Dickinson, L. A., Gulizia, R. J., Trauger, J. W., Baird, E. E., Mosier, D. E., Gottesfeld, J. M. and Dervan, P. B. (1998) *Proc. Natl. Acad. Sci. U. S. A.* **95,** 12890-12895.

18. Wurtz, N. R., Pomerantz, J. L., Baltimore, D. and Dervan, P. B. (2002) *Biochemistry* **41,** 7604-7609.

19. White, S., Szewczyk, J. W., Turner, J. M., Baird, E. E. and Dervan, P. B. (1998) *Nature* **391,** 468-471.

20. Kielkopf, C. L., White, S., Szewczyk, J. W., Turner, J. M., Baird, E. E., Dervan, P. B. and Rees, D. C. (1998) *Science* **282,** 111-115.

21. Dervan, P. B. and Edelson, B. S. (2003) *Curr. Opin. Struct. Biol.* **13,** 284-299.

22. Foister, S., Marques, M. A., Doss, R. M. and Dervan, P. B. (2003) *Bioorg. Med. Chem.* **11,** 4333-4340.

23. Tischer, E., Mitchell, R., Hartman, T., Silva, M., Gospodarowicz, D., Fiddes, J. C. and Abraham, J. A. (1991) *J. Biol. Chem.* **266,** 11947-11954.

24. Belitsky, J. M., Nguyen, D. H., Wurtz, N. R. and Dervan, P. B. (2002) *Bioorg. Med. Chem.* **10,** 2767-2774.

25. Trauger, J. W. and Dervan, P. B. (2001) *Methods Enzymol*. **340,** 450-466.

26. Wood, S. M. and Ratcliffe, P. J. (1997) *Int J. Biochem. Cell Biol.* **29,** 1419-1432.

27. Bianchi, L., Tacchini, L. and Cairo, G. (1999) *Nucl. Acids. Res.* **27,** 4223-4227.

28. Aerts, J. L., Gonzales, M. I. and Topalian, S. L. (2004) *Biotechniques* **36,** 84-86, 88, 90-91.

29. Hung, C. J., Ginzinger, D. G., Zarnegar, R., Kanauchi, H., Wong, M. G., Kebebew, E., Clark, O. H. and Duh, Q. Y. (2003) *J. Clin. Endocrinol. Metab.* **88,** 3694-3699.

30. Nelson, J., Bagnato, A., Battistini, B. and Nisen, P. (2003) *Nat. Rev. Cancer* **3,** 110-116.

31. Grimshaw, M. J., Naylor, S. and Balkwill, F. R. (2002) *Mol. Cancer Ther.* **1,** 1273-1281.

32. Soker, S., Gollamudi-Payne, S., Fidder, H., Charmahelli, H. and Klagsbrun, M. (1997) *J. Biol. Chem.* **272,** 31582-31588.

33. Hanahan, D. and Folkman, J. (1996) *Cell* **86,** 353-364.

34. Plate, K. H., Breier, G., Weich, H. A. and Risau, W. (1992) *Nature* **359,** 845-848.

35. Leung, D. W., Cachianes, G., Kuang, W. J., Goeddel, D. V. and Ferrara, N. (1989) *Science* **246,** 1306-1309.

36. Gasparini, G., Toi, M., Gion, M., Verderio, P., Dittadi, R., Hanatani, M., Matsubara, I., Vinante, O., Bonoldi, E., Boracchi, P., Gatti, C., Suzuki, H. and Tominaga, T. (1997) *J. Natl. Cancer Inst.* **89,** 139-147.

37. Kang, S. M., Maeda, K., Chung, Y. S., Onoda, N., Ogawa, Y., Takatsuka, S., Ogawa, M., Sawada, T., Nakata, B., Nishiguchi, Y., *et al*. (1997) *Oncol. Rep.* **4,** 381-384.

38. Kim, K. J., Li, B., Winer, J., Armanini, M., Gillett, N., Phillips, H. S. and Ferrara, N. (1993) *Nature* **362,** 841-844.

39. Lin, P. N., Sankar, S., Shan, S. Q., Dewhirst, M. W., Polverini, P. J., Quinn, T. Q. and Peters, K. G. (1998) *Cell Growth Differ.* **9,** 49-58.

40. Hennequin, L. F., Thomas, A. P., Johnstone, C., Stokes, E. S. E., Ple, P. A., Lohmann, J. J. M., Ogilvie, D. J., Dukes, M., Wedge, S. R., Curwen, J. O., *et al*. (1999) *J. Med. Chem.* **42,** 5369-5389.

41. Shi, W. and Siemann, D. W. (2002) *Br. J. Cancer* **87,** 119-126.

42. Zhang, L., Yang, N., Mohamed-Hadley, A., Rubin, S. C. and Coukos, G. (2003) *Biochem. Biophys. Res. Commun.* **303,** 1169-1178.

43. Reich, S., Fosnot, J., Kuroki, A., Tang, W. X., Yang, X. Y., Maguire, A., Bennett, J. and Tolentino, M. (2003) *Mol. Vis.* **9,** 210-216.

44. Darnell, J. E. (2002) *Nat. Rev. Cancer* **2,** 740-749.

45. Kung, A. L., Wang, S., Klco, J. M., Kaelin, W. G. and Livingston, D. M. (2000) *Nat. Med.* **6,** 1335-1340.

46. Kung, A. L., Zabludoff, S. D., France, D. S., Freedman, S. J., Tanner, E. A., Vieira, A., Cornell-Kennon, S., Lee, J., Wang, B. Q., Wang, J. M., *et al*. (2004) *Cancer Cell* **6,** 33-43.

47. Marti, H. H. and Risau, W. (1998) *Proc. Natl. Acad. Sci. U. S. A.* **95,** 15809-15814.